Applied Catalysis B: Environmental 121–122 (2012) 171–181

Contents lists available at SciVerse ScienceDirect

Applied Catalysis B: Environmental

journal homepage: www.elsevier.com/locate/apcatb

Comparison of the efficiency and mechanism of catalytic ozonation of 2,4,6-trichloroanisole by iron and manganese modified bauxite

Fei Qi[a,*], Bingbing Xu[b], Lun Zhao[a], Zhonglin Chen[c], Liqiu Zhang[a], Dezhi Sun[a], Jun Ma[c]

[a] Research Centre for Water Pollution Source Control and Eco-Remediation, Beijing Key Lab for Source Control Technology of Water Pollution, College of Environmental Science and Engineering, Beijing Forestry University, Beijing, 150090, PR China
[b] State Key Laboratory of Environmental Criteria and Risk Assessment, Chinese Research Academy of Environmental Sciences, Beijing, 100012, PR China
[c] State Key Laboratory of Urban Water Resource and Environment, Harbin Institute of Technology, Harbin 150090, PR China

ARTICLE INFO

Article history:
Received 1 August 2011
Received in revised form 22 March 2012
Accepted 4 April 2012
Available online 11 April 2012

Keywords:
Catalytic ozonation
Bauxite
Iron modification bauxite (IMB)
Manganese modification bauxite (MMB)
2,4,6-Trichloroanisole

ABSTRACT

The efficiency and mechanism of catalytic ozonation of 2,4,6-trichloroanisole (TCA) by metal oxide modified bauxite were studied. TCA was effectively degraded by catalytic ozonation in the presence of iron- or manganese-modified bauxite (IMB or MMB). The effect of water pH on catalytic ozonation indicated that surface property was the key factor that influenced the activity of catalyst. Analysis results of the isoelectric point (IEP) and zeta potential for catalyst further confirmed that a lower zeta potential for modified bauxite enhanced catalytic activity. Results of both catalytic ozone decomposition and radical scavengers experiments indicated that catalytic ozonation by IMB or MMB followed a hydroxyl radical (•OH) reaction pathway. The main reaction pathway was proposed that adsorption of both ozone and TCA in the micropores and subsequent interaction (direct and indirect oxidation) between them that was confirmed by the analysis of the surface pore volume and surface hydroxyl groups, being followed by the diffusion of ozone and TCA on the mesoporous surface, in which surface hydroxyl groups covering mesoporous surface initialed ozone decomposition to generate •OH, resulted in TCA degradation.

1. Introduction

2,4,6-Trichloroanisole (TCA) as a pollutant in water can cause unpleasant taste and odor in tap water [1]. It is generated from chlorophenol by microorganisms in the distribution system of drinking water [2]. Moreover, TCA may also be intermittently released into surface water or underground water by industrial processes such as wine industry [3,4] and wood industry [5]. Because it contains chlorine atom in its molecule structure, TCA is toxic to humans [6]. Consequently, the occurrence of TCA in source water and tap water is of concern to the public.

Because of its low molecular weight and special chemical structure, TCA is not effectively removed from source water by the conventional water treatment that includes coagulation, sedimentation, filtration, and disinfection [7]. In recent years, several pre-treatments and advanced treatments have been used to enhance the removal efficiency of TCA from drinking water [8,9]. In the 1980s, pre-oxidation (including potassium permanganate, chlorination, or ozonation) has been introduced to conventional drinking water treatment to promote TCA degradation [10]. Because of a low oxidation–reduction potential, potassium permanganate cannot remove TCA from water effectively. Chlorination also cannot remove TCA effectively, but can produce some by-products such as chloroform, bromoform, chlorophenol and bromophenol [11–13]. These disinfection by-products are much toxic for humans. Ozonation as pre-oxidation or advanced oxidation in drinking water treatment can efficiently remove TCA [11]. However, some by-products such as bromate, ketoaldehyde and ketone acid can be generated in ozonation [14] and natural organic matters (NOMs) had great negative effect on the removal efficiency of ozonation [15]. Several researchers have focused on TCA removal from drinking water by activated carbon (AC) including powdered AC (PAC) and granular (GAC) [9,10]. Although AC effectively adsorbs TCA from drinking water, a large mass of AC is required to maintain high removal efficiency. This treatment generates a large quantity of residual AC sludge that needs to be processed.

Some advanced water treatments including membrane processes and advanced oxidation processes (AOPs) have been investigated for developing the removal efficiency of TCA. Ultrafiltration, nanofiltration and reverse osmosis can remove TCA from water efficiently [2]. However, both the manufacture cost and membrane fouling limit the application of membranes in water treatment plants. AOPs that involve the generation of hydroxyl radical (•OH) as the predominant species for the degradation of micropollutants, are attractive alternatives and have received

* Corresponding author at: P.O. Box 60, No. 35 Qinghua East Road, Haidian District, Beijing, PR China. Tel.: +86 10 62336596; fax: +86 10 62336596.
E-mail addresses: qifei@bjfu.edu.cn, qifei_hit@yahoo.com.cn (F. Qi).

0926-3373/$ – see front matter © 2012 Elsevier B.V. All rights reserved.
http://dx.doi.org/10.1016/j.apcatb.2012.04.003

considerable attention in recent years. Several AOPs, such as catalytic ozonation [14], photocatalytic degradation [3] and gamma radiation [15], have been used for the removal of TCA from water with satisfactory results.

Catalytic ozonation by the solid catalyst exhibits the significant removal efficiency for organic pollutants in drinking water and wastewater. Catalytic ozonation promotes ozone decomposition to generate •OH in the presence of catalysts. Because of requiring no additional chemicals, simple application and high removal efficiency, heterogeneous catalytic ozonation has been focused by researchers in recent years. Catalysts most widely used in heterogeneous catalytic ozonation are metal oxides, metals on supports, minerals modified with metals, and AC. Many metal oxides such as MnO_2 [16], TiO_2 [17], CeO_2 [18], aluminum oxides [7,14,19,20] and iron oxides [21,22] have been used as catalysts. To enhance the mechanical ability of the catalyst, metals and metal oxides are coated on supports or minerals. In our previous research, the efficiency and mechanism of TCA removal by catalytic ozonation with aluminum oxides (γ-AlOOH, γ-Al_2O_3 and α-Al_2O_3) have been systematically investigated [7,21].

Natural bauxite is an inexpensive and environmental friendly mineral with moderate solubility in water. Because of its low cost and stability, the bauxite is popular in catalytic reactions as a support. In our previous research, raw or thermally treated bauxite was used as the catalyst in heterogeneous catalytic ozonation to remove TCA and 2-methylisoborneol (MIB) from water [11,21]. The raw bauxite exhibited catalytic activity in ozonation of TCA, and thermal treatment enhanced the catalytic activity of bauxite in ozonation of MIB. These investigations were focused on taste and odor problems in drinking water. Generally, the concentration of TCA released into the natural water system by industrial processes is present at μg/L level. Consequently, it is of interest to determine if catalytic ozonation by bauxite can remove TCA with high concentrations in water. According to previous research results, the degradation efficiency of TCA by catalytic ozonation by raw or thermal treated bauxite was significantly affected by the initial concentration of TCA (or MIB). Therefore, there are some problems with catalytic ozonation by bauxite. To enhance the performance, decreasing the dosage of ozone and catalyst used in TCA removal and modification of raw bauxite are necessary.

Manganese oxide [23–25] and iron oxides [26,27] exhibited significant activity in catalytic ozonation because of their unique surface properties. In this study, the modification by manganese oxides or iron oxides for raw bauxite was carried out. Moreover, the catalytic active site and surface properties are keys to enhancing the catalytic activity. However, only several studies focused the role of pore or surface function group in reaction mechanism of catalytic ozonation. To reveal the role of pore or surface function group in catalytic ozonation is important for understanding the reaction mechanism. The aim of this study is to develop the catalytic activity of bauxite by the modification with metal oxides and to discuss the catalytic reaction mechanism. To simulating the real water quality contaminated by industry wastewater, the concentration of TCA is controlled at μg/L. The degradation efficiencies with iron and manganese modified bauxite are compared. Differences in the surface textures and chemical characteristic of the catalysts are identified to investigate the role of surface properties in the catalytic ozonation, and to discuss the catalytic reaction mechanism.

2. Materials and methods

2.1. Chemicals

Raw bauxite mineral was purchased from Baise City (Guang Xi Province, China). TCA was obtained from Tokyo Kasei Kogyo Co. Ltd. (Tokyo, Japan) and the purity >95%. The stock solution was prepared by directly dissolving TCA in ultra-pure water (≥18.0 MΩ cm) produced with a Milli-Q system (Millipore, France). Chromatogram grade *n*-pentane was purchased from Sigma–Aldrich (USA), and was used to extract TCA from water for analysis. Other reagents such as manganese acetate, $Fe(NO_3)_3$, $Ce(NO_3)_3$, NaOH, KH_2PO_4, Na_2SO_3 and H_3PO_4 were all of analytic grade and were used without further purification.

2.2. Preparation of modified catalyst

Modified bauxite was prepared by incipient wetness impregnation. The wetness impregnation means that the raw bauxite was dropped into a manganese acetate ($Mn(CH_3COO)_2$) or iron nitrate ($Fe(NO_3)_3$) solution. Detailed optimized preparation information was below. Firstly, the raw bauxite powder was washed with ultra-pure water more than three times to remove surface dust, and then was crushed and sieved to obtain 0.075–0.3 mm particles. Secondly, the crushed raw bauxite was modified by the incipient wetness impregnation method with aqueous solutions of the metal salts (0.2 mol/L, 100 mL) with an impregnation time of 16 h. After that, the suspension was then filtrated and washed until the pH and conductivity of supernatant maintained at a constant. Then, the solid samples were dried at 70 °C for 48 h before the calcination at 600 °C for 4 h in air. After the calcination, the modified bauxite samples were cooled to room temperature. The powder was the optimization catalyst.

In experiments of optimization preparation conditions for IMB or MMB, precursor ($Mn(CH_3COO)_2$ or $Fe(NO_3)_3$ solution) concentration, impregnating time and calcination temperature were optimized.

2.3. Catalytic ozonation

The catalytic ozonation with or without the catalysts was performed in batch mode at ambient temperature in a glass reactor (1 L) that had been produced from a flat-bottomed flask. The solution and the catalyst were mixed by a magnetic stirrer. The reaction system has been described previously [7]. Ozone was produced by a laboratory ozonizer (3S-A5, Beijing Tonglin Gaoke Technology, Beijing, China) supplied with dry pure oxygen. The maximum ozone production was 5.0 g/h. After the generator reached a steady state, ozone gas was bubbled into ultra-pure water in the reactor with a silica dispenser to reach the desired dissolved ozone concentration. Then, the ozone gas supply was shut off. After that, the catalysts and TCA stock solution (1 mL) were immediately introduced into the reactor, and the magnetic stirrer was turned on. Samples were collected from the reactor at specific times. Before analysis, samples were filtered with cellulose acetate filters (0.45 μm) for the separation of catalyst particles. In this reaction system, ozone was introduced to the system once, and the concentrations of aqueous ozone and TCA decreased during the reaction. A sealed reactor was used to eliminate volatilization of aqueous ozone and TCA. The oxygen flux, time when ozone was introduced, and the voltage for ozone production were varied to adjust the initial concentration of the dissolved ozone. The solution pH was maintained at 6.5 by adjustment with phosphate buffer solution (0.1 mmol/L). Adsorption experiments were carried out in the same reactor using N_2 instead of O_3. To obtain valid data, experiments were repeated three times, and data were averaged.

Experiments of evaluating the dissolution of metal ions from catalyst were carried out in the same reactor above. And the experiment procedure was the same as catalytic ozonation. Samples collected from the reactor were analyzed by inductive coupled

plasma-atomic emission spectroscopy (ICP-AES, Optima 7300DV, Perkin Elmer, USA).

2.4. Analysis methods

2.4.1. Characterization of catalysts

Scanning electron microscopy (SEM, Hitachi S-3400, Japan) was used for imaging. Prior to SEM measurements, the samples were mounted on a platform using PVC glue and then sputter coated with gold. The plate holding the sample was placed in the electron microscope for analysis at magnifications of 300 and 6000. Surface texture characteristics of catalysts were determined from nitrogen adsorption isotherms at 77 K on a surface area and porosity analyzer (ASAP 2020M, Micromeritics, USA). First, samples were degassed at 250 °C for 24 h under a residual vacuum of less than 10^{-4} Pa before analysis. And then, the nitrogen adsorption isotherms were analyzed according to Dubinin's theory. The specific surface area was calculated by BET model. The total volume (V_{tot}) was calculated by Kelvein model and the micropore volume (V_{micro}) was speculated by *t*-plot model. The mesopore volume (V_{meso}) was calculated by $V_{tot} - V_{micro}$. Infrared spectra of catalysts were measured using a Fourier transform infrared (FT-IR) spectrum instrument (Spectrum One, Perkin Elmer, USA) using KBr disc method. The iron and manganese concentrations of the catalyst were analyzed by ICP-AES following acid digestion of the catalysts.

2.4.2. Analysis of aqueous ozone and TCA

The dissolved ozone concentration was measured colorimetrically by the indigo method [28].

A sample of aqueous TCA (25.0 mL) was extracted by *n*-pentane (1.0 mL) and analyzed by gas chromatogram– mass spectrum (GC–MS, GC7890-MS5975, Agilent, USA) in selected ion monitoring mode (SIM), which was modified according to Shin and Ahn [29]. Each water sample (20.0 mL) was placed in a 25.0 mL separatory funnel, and 2.0 g of KH_2PO_4 and 3.0 g of NaCl were added into the solution. The sample was extracted with 1.0 mL of *n*-pentane by mechanical shaking for 5.0 min. The organic phase was dried with anhydrous sodium sulfate and transferred to an autosampler vial. At appropriate times, a 1.0 μL aliquot of the solution was injected into the GC system. All mass spectra were obtained with the Agilent GC7890-MS5975 instrument. The ion source was operated in the electron ionization mode (electron energy 70 EV, 230 °C). Full scan mass spectra were recorded for identification of the analytes at the high concentration. Trace chemicals were confirmed using two characteristic MS ions and matching GC retention time. The ions selected for TCA in this investigation were *m*/*z* 195 and *m*/*z* 196. The detection limit was 0.4 μg/L and the relative standard deviation was below 5.3%. The experiments were conducted in triplicate, and averaged data are shown in this study.

3. Results and discussion

3.1. Catalytic activity of metal oxide modified bauxite

In this study, bauxite was modified with metal salts such as Mn(II), Ce(III) or Fe(III). In general, these metal oxides are active species in catalytic ozonation for removing pollutants [27,30,31]. The catalytic activities of the modified bauxites were tested and results are shown in Fig. 1.

The degradation efficiency of TCA was only 55.8% in the sole ozonation. The low-level ozone dose could not remove TCA efficiently in this short reaction time. By comparison, the degradation efficiency of TCA was enhanced by catalytic ozonation of raw bauxite (degradation efficiency was 72.4%). Compared with our previous study [14], the degradation efficiency for a high concentration solution of TCA by catalytic ozonation with the raw bauxite (in this study) was much lower than that for a low concentration solution of TCA (in previous study).

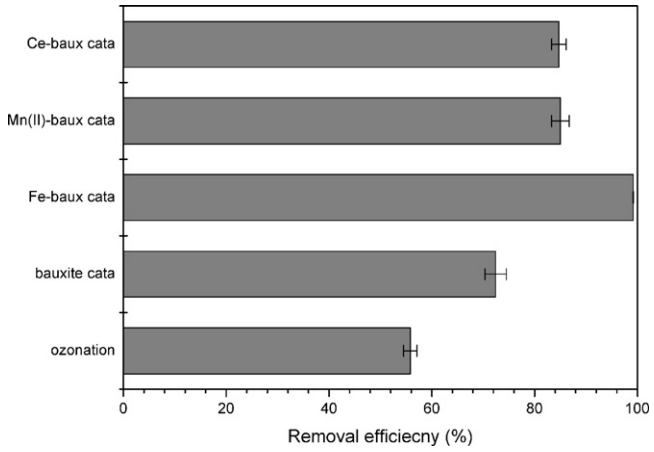

Fig. 1. Catalytic activity of bauxite modified by different metal oxides in catalytic ozonation. Experiment conditions were: $[TCA]_0 = 28.2$ μg/L, $[O_3]_0 = 0.62$ mg/L, $[catalyst]_0 = 500$ mg/L, solution pH 6.5 adjusted with phosphate buffer solution, and the reaction time 60 min.

According to Fig. 1, all modification of bauxite enhanced the degradation efficiency of TCA. Iron modification achieved the best degradation efficiency and >99.0% of TCA degraded. Compared with the sole ozonation, the degradation efficiency of TCA was enhanced 38.1%. After 60 min reaction, the degradation efficiency of TCA was 85.02% for MMB and 84.72% for Ce(III) modified bauxite, respectively. Among all the modified bauxites, IMB had the greatest catalytic activity compared.

Iron oxides and manganese oxides have been reported to be high effectiveness catalysts that exhibit good catalytic activity in catalytic ozonation [23,32,33]. In this study, iron or manganese oxide was used to modify raw bauxite. After modification, metal oxides may cover the surface of the raw bauxite. Modification with iron or manganese oxide changed the surface properties of the bauxite resulted in the development of the catalytic activity. Moreover, both the solubility of the iron and manganese oxides was lower than those of other metal oxides. Therefore, subsequent studies on the optimization of preparation conditions, the catalytic reaction kinetics, and characterization of physical and chemical properties catalyst focused on the iron and manganese modified bauxite.

3.2. Optimization of metal oxide modification condition

All of the concentration of metal salt, the impregnation time, and the calcination temperature were critical parameters for modified bauxite preparation. These preparation conditions were optimized and the results are shown in Table 1. For IMB, the optimized parameters were 0.2 mol/L for $Fe(NO_3)_3$ concentration, 16 h for impregnation, and 600 °C for calcination. For MMB, the optimized parameters were 0.2 mol/L for $(C_2H_3O_2)_2Mn$ concentration, 4 h for impregnation, and 400 °C for calcination. In experiments of degradation efficiency, reaction kinetics, catalytic reaction mechanism in this study, catalyst used in catalytic ozonation was prepared under optimized parameters.

3.3. Effect of the metal oxide mass on the catalytic activity

In Section 3.2, the mass fraction of the catalyst was observed to have a large effect on the catalytic activity. In this section, the

Table 1
Optimization of preparation condition of modified bauxite by Fe or Mn.

Catalyst	Concentration of $Fe(NO_3)_3$ or $(C_2H_3O_2)_2Mn$ (mol/L)	Impregnating time (h)	Calcination temperature (°C)	Removal efficiency (%)
Catalyst-Fe-1	0.08	16	600	90.43
Catalyst-Fe-2	0.12	16	600	91.55
Catalyst-Fe-3	0.2	16	600	92.97
Catalyst-Fe-4	0.3	16	600	85.55
Catalyst-Fe-5	0.4	16	600	75.81
Catalyst-Fe-6	0.2	4	600	64.61
Catalyst-Fe-7	0.2	8	600	75.33
Catalyst-Fe-8	0.2	12	600	89.08
Catalyst-Fe-10	0.2	20	600	76.91
Catalyst-Fe-11	0.2	16	200	70.50
Catalyst-Fe-12	0.2	16	300	76.72
Catalyst-Fe-13	0.2	16	400	78.64
Catalyst-Fe-14	0.2	16	600	84.51
Catalyst-Mn-1	0.08	16	600	81.70
Catalyst t-Mn-2	0.12	16	600	84.00
Catalyst t-Mn-3	0.2	16	600	85.00
Catalyst t-Mn-4	0.3	16	600	69.90
Catalyst t-Mn-5	0.4	16	600	71.30
Catalyst t-Mn-6	0.2	4	600	85.00
Catalyst t-Mn-7	0.2	8	600	72.76
Catalyst t-Mn-8	0.2	16	600	75.11
Catalyst t-Mn-10	0.2	18	600	69.72
Catalyst t-Mn-11	0.2	4	200	62.59
Catalyst t-Mn-12	0.2	4	300	68.86
Catalyst t-Mn-13	0.2	4	400	85.00
Catalyst t-Mn-14	0.2	4	600	77.56

Reaction condition: $[TCA]_0$ = 28.2 μg/L, $[O_3]_0$ = 0.62 mg/L, $[catalyst]_0$ = 500 mg/L, solution pH 6.5 adjusted with phosphate buffer solution, the reaction time was 40 min.

effect of the catalyst mass on the catalytic activity was investigated further.

Fig. 2 shows the effect of loaded mass content on catalytic ozonation of TCA with an ozone dosage of 0.62 mg/L. A maximum TCA degradation efficiency of 90.0% was obtained after 40 min of catalytic ozonation when the concentration of $Fe(NO_3)_3$ was 0.2 mol/L. The effect of the iron loading content on the degradation efficiency was obvious, and the corrected iron loading mass was essential for development of catalytic activity. There was an inflection point in the figure for this effect on TCA degradation efficiency. Insufficient or excess iron loading content was not good for the catalytic activity. For MMB, when the concentration of $(C_2H_3O_2)_2Mn$ was 0.2 mol/L, the maximum degradation efficiency of TCA was 90.0%. There was also an inflection point in the figure for this effect on TCA degradation efficiency. As the same as IMB, insufficient or excess Mn loading was not good for catalytic activity in the modification of raw bauxite.

Generally, loading content of metal oxide in the catalyst increased with the increasing concentration of the precursor solution. This increase altered the specific surface area and total pore volume of the catalyst. As iron oxide or manganese oxide grew on the surface of the raw bauxite, the mean pore diameters of IMB and MMB decreased. This illustrated that an increased mass fraction of iron oxide or manganese oxide enhanced steric hindrance and decreased the mean pore diameter of the catalyst, which was not favorable for catalytic activity. Moreover, iron oxide or manganese oxide on the surface of the raw bauxite was essential for catalytic ozonation. In previous studies, iron oxides (Fe_2O_3, FeOOH [21,22]) and manganese oxide [23,25] have been shown to promote ozone decomposition to •OH. However, the dosage of iron oxide or manganese oxide obviously affected the pollutant degradation efficiency. Excess catalyst was not good for the pollutant removal. Excess metal oxides enhanced ozone decomposition to generated •OH in excess, resulted in •OH quenching. These results agree with the experimental data obtained in this study for the effect of loaded mass of metal on the catalytic activity.

3.4. Reaction kinetics of catalytic ozonation by IMB and MMB

In catalytic ozonation, organic pollutants are removed by a combination reaction, including direct ozonation, surface adsorption by catalyst, and catalytic ozonation. Investigation of the contributions of each reaction to the degradation of organic pollutants can be used to study the mechanism and kinetics of the catalytic ozonation. The results for the degradation efficiency of TCA by sole ozonation, and the adsorption and catalytic ozonation by raw bauxite, IMB and MMB are shown in Fig. 3.

According to Fig. 3, the degradation efficiency of TCA by adsorption on catalyst was weak for raw bauxite, IMB and MMB. The adsorption behaviors of TCA on raw bauxite and modified bauxite (IMB and MMB) were quite different. TCA was adsorbed rapidly on all three catalysts. The adsorption of TCA on both IMB and MMB was higher than that on raw bauxite. The saturation adsorption time was extended to 60 min in TCA adsorption by modified bauxite (IMB and MMB). The adsorption of TCA on IMB was less than that on MMB. Modification by iron or manganese developed the surface properties of raw bauxite, which enhanced for the adsorption of TCA.

The introduction of raw bauxite, IMB and MMB into the ozonation process enhanced the degradation efficiency of TCA from water. Modification with iron and manganese increased the catalytic activity of raw bauxite. The degradation efficiency of TCA was >99.0% after IMB catalytic ozonation, and was increased 71.3% compared with the sole ozonation. For catalytic ozonation with MMB, the degradation efficiency of TCA was 85.02%, which was increased almost 57% compared with the sole ozonation. For IMB and MMB, the degradation efficiencies of TCA by adsorption were all <10.0%, which indicates that the catalytic reaction play an important role in catalytic ozonation by IMB and MMB.

Because of the lower initial concentration of TCA at the level of the actual surface water or industry wastewater, it was difficult for the qualitative or quantitative analysis of by-products with much lower concentrations. Therefore, to evaluate the safety of treated water by the concentration of by-products below the legal limits

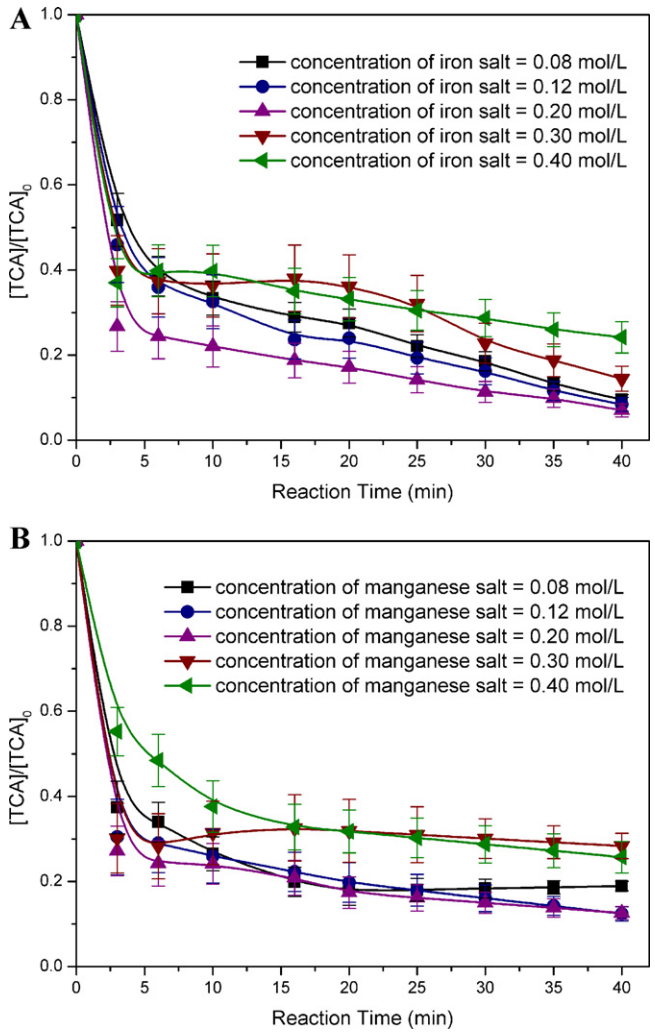

Fig. 2. Effect of loaded mass on degradation efficiency of TCA. Experiment conditions were: $[TCA]_0 = 28.2\ \mu g/L$, $[O_3]_0 = 0.62$ mg/L, $[catalyst]_0 = 500$ mg/L, solution pH 6.5 adjusted with phosphate buffer solution, reaction time 40 min, (A) iron modification, (B) manganese modification.

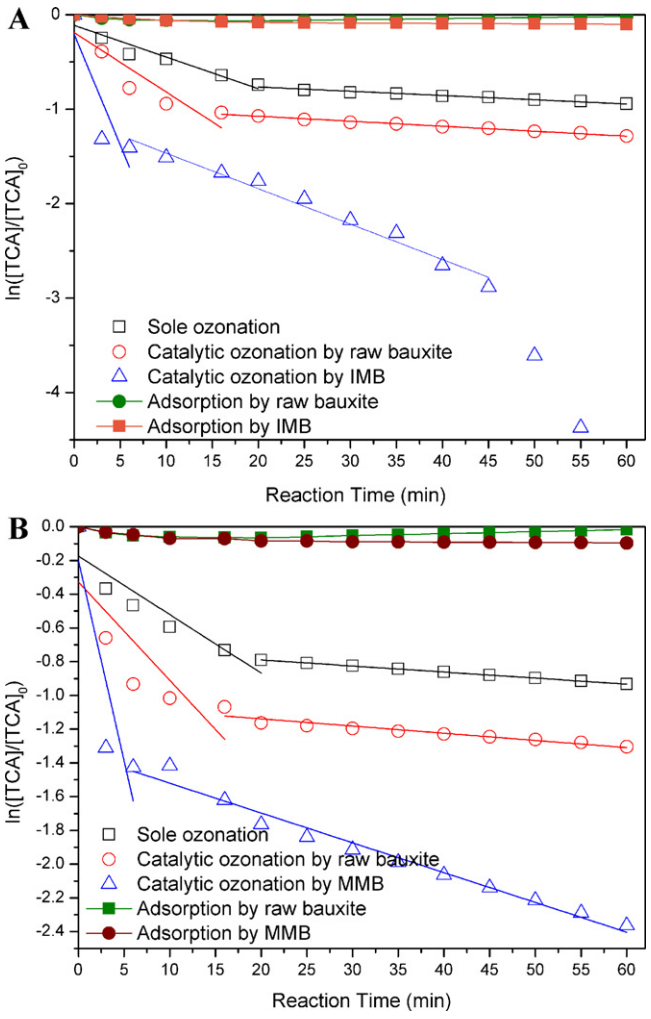

Fig. 3. Degradation kinetics for TCA by catalytic ozonation in the presence of the raw bauxite, IMB and MMB. Experiment conditions were: $[TCA]_0 = 28.2\ \mu g/L$, $[O_3]_0 = 0.62$ mg/L, $[catalyst]_0 = 500$ mg/L, the concentration of precursor was 0.2 mol/L for IMB or MMB, solution pH 6.5 adjusted with phosphate buffer solution, reaction time 60 min, (A) IBM catalytic ozonation, (B) MMB catalytic ozonation.

was impossible. In this study, the mineralization performance was used to evaluate the safety of treated water. The high mineralization performance of IMB and MMB were also exhibited with different ozone dosages, results shown in Fig. S1. According to the high performance on TCA removal and mineralization, the modification of bauxite by iron or manganese is good for development the catalytic activity. The high mineralization performance made IMB be a good catalyst in drinking water treatment.

In the ozonation system, the model compound is usually decomposed by direct and indirect reaction pathways [13]. The direct reaction is of the model compound with molecular ozone, and the indirect reaction is decomposition of the model compound by •OH [34]. The kinetics of catalytic ozonation is assumed to fit second-order or pseudo-first-order, which was also carried out in several previous studies [33,35]. In this investigation, the degradation rate of TCA in both ozonation and catalytic ozonation by raw bauxite, IMB and MMB can be expressed as follows:

$$-\frac{d[TCA]}{dt} = k_{O_3}[O_3][TCA] + k_{\bullet OH}[\bullet OH][TCA] \quad (1)$$

where k_{O_3} and $k_{\bullet OH}$ are constants for ozone and •OH reacting with TCA, respectively. Eq. (1) can be transformed to Eq. (2).

$$-\frac{d[TCA]}{dt} = (k_{O_3}[O_3] + k_{\bullet OH}[\bullet OH])[TCA] \quad (2)$$

By defining $k_{app} = k_{O_3}[O_3] + k_{\bullet OH}[\bullet OH]$, Eq. (2) can be transformed to Eq. (3).

$$-\frac{d[TCA]}{dt} = k_{app}[TCA] \quad (3)$$

As shown in Eq. (3), the degradation rate of TCA in both ozonation and catalytic ozonation by raw bauxite, IMB or MMB could be predigested as pseudo-first order. Plots of $\ln([TCA]/[TCA]_0)$ versus the reaction time of the sole ozonation and catalytic ozonation by raw bauxite, IMB or MMB are shown in Fig. 3. A good linear fitting was observed for each of these ozonation reactions. This indicated that TCA degradation in both ozonation and catalytic ozonation was described by the pseudo-first order as shown in Eq. (3). A two-stage reaction occurred in both the sole ozonation and catalytic ozonation (Fig. 2). The initial stage, called instantaneous ozone demand (IOD), was explained by the fast consumption of ozone by organic pollutants in water or by the catalyst (the raw bauxite or IMB) [36,37]. In the stage of IOD, a fast oxidation reaction between ozone (or •OH) and TCA took place. According to the results, the IOD stage

Table 2
Pseudo-first-order rate constants of TCA degradation in the different processes.

Experiments	Kinetics constants (min^{-1})		R^2	
	The initial phase	The second phase	The initial phase	The second phase
Ozonation	0.0336	4.50×10^{-3}	0.9245	0.9704
Catalyzed ozonation by raw bauxite	0.0498	5.00×10^{-3}	0.7737	0.9938
Catalyzed ozonation by IMB	0.2340	69.20×10^{-3}	0.7970	0.9084
Catalyzed ozonation by MMB	0.2376	17.7×10^{-3}	0.8100	0.9785

reaction followed pseudo-first-order kinetics. The second stage was a slow oxidation process where residual ozone molecular continued to oxidize TCA. In catalytic ozonation, the residual ozone can be decomposed by the catalyst, which generates active oxygen species that can degrade TCA more efficiently. The reaction in the second stage also followed pseudo-first-order kinetics. The pseudo-first-order kinetic parameters are listed in Table 2. In both the initial stage and the second stage, IMB exhibited better catalytic than MMB activity in catalytic ozonation of TCA.

Furthermore, the reaction time for the first stage of the sole ozonation, catalytic ozonation by raw bauxite, and catalytic ozonation by modified bauxite were quite different. For the sole ozonation, the first stage time was 20 min. In catalytic ozonation, the first stage was shorter than that of the sole ozonation, being 15 min and 7 min for catalytic ozonation by raw bauxite and modified bauxite, respectively. This shortening of first stage time indicated that the reaction rate of ozone and TCA was faster when initiated by the catalyst. This phenomenon was consistent with the results for TCA degradation efficiency and confirmed that the catalytic reaction took place after the introduction of raw bauxite and modified bauxite.

3.5. Effect of pH on the catalytic activity of modified bauxite

Water pH is one of the most important factors in the ozone decomposition process. Hydroxide ions (OH^-) were found to be the initiator of the chain reaction in ozone decomposition [38]. Water pH reflects its concentration of OH^-. The rate of ozone decomposition increases with increasing pH, which promotes the formation of •OH. The water pH is also one of the most important factors affecting the surface properties of oxides [39]. Therefore, the effect of pH on the catalytic activity of modified bauxite can be used to evaluate the removal efficiency and catalytic reaction mechanism.

The effect of water pH on the rate of catalytic ozonation of TCA by raw bauxite or modified bauxite was studied (Fig. 4). From pH 2.0–11.0 for all the catalysts, the catalytic activity increased until pH 9.0 and then decreased.

When the pH was <5.0, the reaction kinetic rate constant for MMB was higher than that of IMB. When the pH was >5.0, the reaction kinetic rate constant for IMB was higher than that of MMB. At lower pH (pH < 5.0), MMB exhibited more significant catalytic activity. However, IMB exhibited remarkable catalytic activity at higher pH (pH > 5.0). This result was caused by two side reasons. Firstly, some element in bauxite or modified bauxite released cation ions under a certain water pH. The dissolution of the element made active species losing in catalyst, resulting in the decreasing of the reaction kinetic rate constant. The dissolution of the element existed when water pH was lower than 6.0 or higher than 8.5. The second reason was the change of catalyst surface property. The surface properties of the catalyst were important in determining the effect of water pH on the catalytic activity. To characterize the surface acid–basic properties of raw and modified bauxites, zeta potential analysis was carried out (Fig. 5). The isoelectric points (IEPs) for raw bauxite, MMB and IMB were 1.61, 1.62 and 2.53, respectively. According to IEPs, the surface acidity of catalyst could be determined, and the order of surface acidity was raw

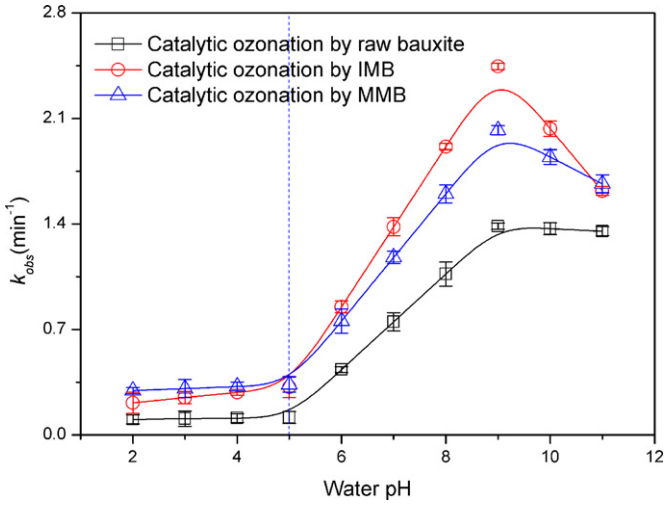

Fig. 4. Effect of water pH on the catalytic activity of raw bauxite or modified bauxite. Experiment conditions were: $[TCA]_0 = 28.2\ \mu g/L$, $[O_3]_0 = 0.62\ mg/L$, $[catalyst]_0 = 500\ mg/L$, the concentration of precursor was 0.2 mol/L for IMB or MMB, solution pH adjusted with phosphate buffer solution, reaction time 40 min.

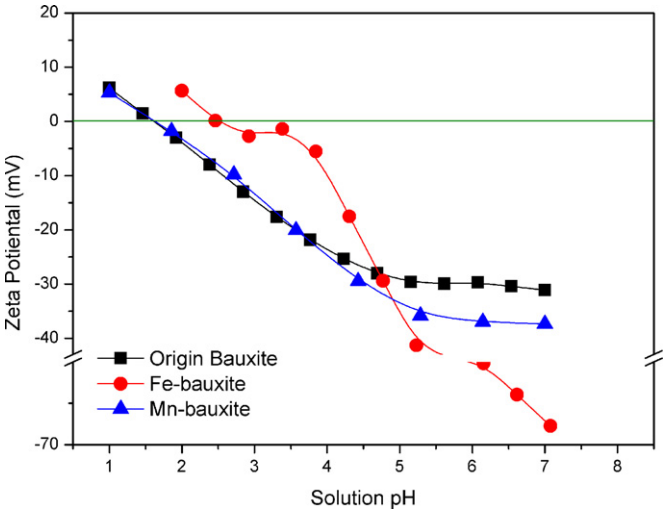

Fig. 5. Zeta potential of raw and modified bauxites.

bauxite > MMB > IMB. The stronger acidity of MMB accounted for the higher catalytic activity when water pH was <5.0. The weaker acidity of IMB accounted for the higher catalytic activity when water pH was >5.0. The surface acid–base properties of the raw and modified bauxites determined the catalytic activity. When the pH was acidity, an acid surface for the modified bauxite was favorable for catalytic ozonation. Otherwise, a basic surface was favorable for catalytic activity.

When water pH was <5.0, the zeta potential of MMB was lower than that of IMB, and when water pH was >5.0, the zeta potential of MMB was higher than that of IMB. According to the effect of the pH on the catalytic activity with the different catalysts, the lower zeta

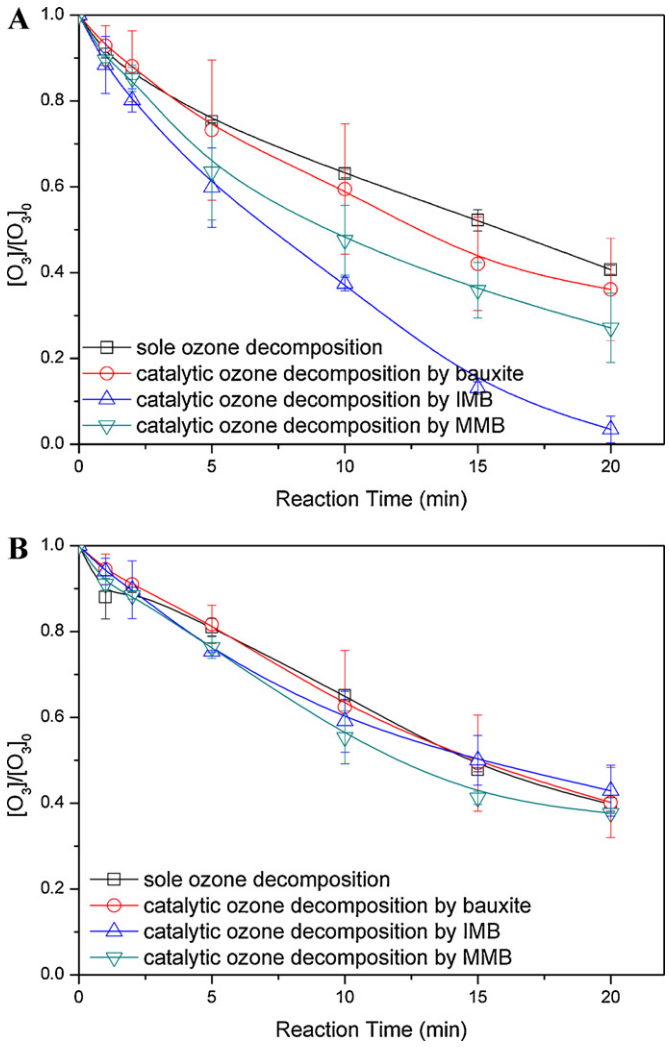

Fig. 6. Catalytic ozone decomposition by modified bauxite. Experiment conditions were: $[O_3]_0$ = 0.62 mg/L, $[catalyst]_0$ = 500 mg/L, the concentration of precursor was 0.2 mol/L for IMB or MMB, solution pH 6.5 adjusted with phosphate buffer solution, reaction time 40 min, (A) without TBA, (B) with TBA (50 mg/L).

potential was another key reason why the catalytic activity of MMB was higher than that of IMB when water pH was <5.0. As the same, the lower zeta potential accounted for the higher catalytic activity of IMB compared to MMB when water pH was >5.0. Therefore, the lower zeta potential of raw or modified bauxite was favorable for the catalytic activity.

3.6. Catalytic ozone decomposition by modified bauxite

Although the degradation efficiency of TCA by catalytic ozonation was significantly increased by the modification of the bauxite, how the catalysts enhanced aqueous ozone decomposition by allowing the formation of active species in the catalytic reaction was not clear. In general, the key active species in catalytic ozonation was •OH. Variation of the ozone decomposition rate can be used as an indirect method to determine whether •OH is generated in catalytic ozonation. Therefore, the ozone decomposition rate by raw bauxite and modified bauxite was observed (Fig. 6).

Raw bauxite exhibited minimal catalytic activity for ozone decomposition (Fig. 6A). Surface modification of the raw bauxite enhanced the efficiency and the reaction rate of catalytic ozone decomposition. Among three catalysts, the order of catalytic activity for catalytic ozone decomposition was IMB > MMB > raw

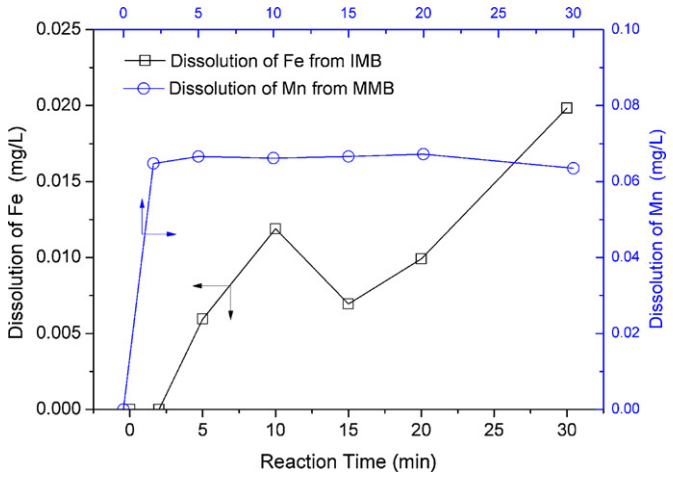

Fig. 7. Dissolution of iron or manganese in the catalytic ozonation. Experiment conditions were: $[TCA]_0$ = 28.2 μg/L, $[O_3]_0$ = 0.62 mg/L, $[catalyst]_0$ = 500 mg/L, the concentration of precursor was 0.2 mol/L for IMB or MMB, solution pH 6.5 adjusted with phosphate buffer solution, reaction time 30 min.

bauxite. This order was consistent with the degradation efficiency order of TCA by catalytic ozonation of these three catalysts. Therefore, the catalytic activity of modified bauxite was account for ozone decomposition that resulted in the degradation of TCA. Ozone decomposition can generate •OH and other active species. To confirm the formation of •OH, inhibition experiments with *tert*-butyl alcohol (TBA) were carried out (results shown in Fig. 6B). Catalytic ozone decomposition was greatly inhibited in these experiments with raw bauxite or modified bauxite. After the introduction of TBA, the final reaction rates of ozone decomposition for the sole ozone decomposition and catalytic ozone decomposition by raw bauxite and modified bauxite were as the same. This result indicates that ozone decomposition was completely inhibited by TBA (50 mg/L). The inhibition effect was in the order IMB > MMB > raw bauxite. This inhibition effect with TBA was consistent with the ability of the catalysts for catalytic ozone decomposition, which indicates that the catalyst with a greater ability for catalytic ozone decomposition could generate more •OH in catalytic ozonation. Therefore, the ability of the three catalysts to catalytic ozone decomposition to generate •OH was in the order IMB > MMB > raw bauxite. This result explained the higher catalytic activity of IMB in the catalytic ozonation of TCA compared to the other catalysts. Surface modification of raw bauxite enhanced the formation of •OH, which can oxidize and remove TCA in water.

3.7. Dissolution of iron or manganese in catalytic ozonation

Modified bauxite was prepared by dipping it into a solution of $Fe(NO_3)_3$ or $(C_2H_3O_2)_2Mn$ and calcination at high temperature. During catalytic ozonation, Fe^{3+} or Mn^{2+} may dissolve in the solution from the modified bauxite surface. The dissolution of Fe^{3+} or Mn^{2+} could be a health risk to humans, and result in homogeneous catalytic ozonation. Therefore, the concentration of dissolved iron or manganese in catalytic ozonation was investigated (results shown in Fig. 7). A small amount of Fe^{3+} dissolved in catalytic ozonation, while the dissolution of Mn^{2+} was higher. As the reaction progressed, the concentration of dissolved Fe^{3+} or Mn^{2+} fluctuated. The dissolution of Fe^{3+} was below the limit in drinking water of China (0.3 mg/L [40]). With compared with the content of iron oxide in IMB, the amount of Fe^{3+} dissolution can be ignored. Therefore, the effect of homogeneous catalytic ozonation by Fe^{3+} is insignificant and the menace of Fe^{3+} dissolution was scarce. In catalytic ozonation by MMB, homogeneous

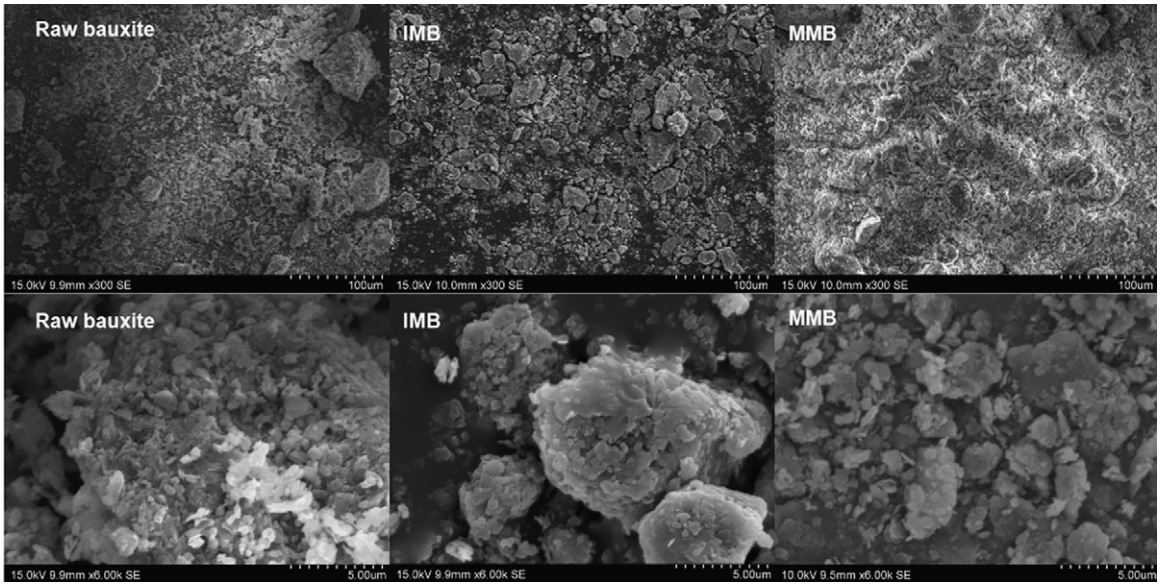

Fig. 8. SEM images of samples of raw bauxite and IMB.

catalytic ozonation occupied a certain proportion. In MMB catalytic ozonation, both homogeneous and heterogeneous reactions took place. The dissolved Mn^{2+} could be oxidized by ozone or OH, which would reduce the level of catalytic active species. This loss would decrease the catalytic activity for organic pollutants. Therefore, the greater dissolution of Mn^{2+} compared to Fe^{3+} could account for the lower catalytic activity of MMB compared to IMB. The dissolution concentration of Mn^{2+} was less than the limit in drinking water in China (0.1 mg/L [40]). The greater dissolution of Mn^{2+} from MMB raised the healthy risk for human. The application of MMB in catalytic ozonation for degradation TCA from water was not safe enough. Therefore, the MMB cannot be used in degradation TCA from drinking water for lower catalytic activity and greater dissolution.

3.8. Surface characterization of raw bauxite, IMB and MMB

The morphologies of the raw bauxite, IMB and MMB were observed at different magnifications by scanning electron microscope (300× and 6000×) (Fig. 8). Significant differences were found among the raw bauxite, IMB and MMB. The raw bauxite, IMB and MMB contained various particles with different sizes (0.5–40.0 μm) and shapes (almost spherical and aggregated). The larger particles observed by SEM might be γ-Al_2O_3. For the raw bauxite, the surface was relatively smooth and flat. After the modification, SEM showed the metal oxides caused the raw bauxite surface being eroded and collapse. The exterior of modified bauxite was rougher than that of raw bauxite, and new cavities appeared in the surface. Modification produced a new surface area and pore volume. Among the catalysts, IMB exhibited the most surface erosion and collapse.

The surface area and the pore volume of the raw bauxite and IMB were investigated using nitrogen adsorption and desorption isotherms, and the BET surface area and pore volume of the catalysts are given in Table 3. Modification of raw bauxite increased the BET surface area and the pore volume of the spherical aggregates. For IMB and MMB, the change in the BET surface area was small, which indicates that the surface area was not the key for enhancing the catalytic activity. The changes in the total pore volume and micropore volume showed that the micropore volume accounted for the increase in the surface area. IMB had the largest micropore volume, and for the different catalysts the micropore volume was in the order IMB > MMB > raw bauxite.

To investigate the surface groups on the catalysts, dry raw bauxite, IMB and MMB samples before use in catalytic ozonation were analyzed by FT-IR (Fig. 9). Interpretation of the FT-IR spectra of the raw bauxite, IMB and MMB was complicated because of the complex compositions of the catalysts. The raw bauxite consisted of several mineral phases with numerous catalytic sites. In the FT-IR spectra of all the catalysts used in this study, the presence of water molecules was supported by the appearance peaks for the bending mode at 1637 cm^{-1} and the stretching mode at 3453 cm^{-1}. The surface hydroxylation resulted in the formation of surface hydroxyl groups on the mineral. After modification, the intensity of surface hydroxyl group peaks (1637 cm^{-1} and 3453 cm^{-1}) increased.

In all spectra, a bond shoulder between 1200 and 990 cm^{-1} was characteristic of aluminosilicate (Al(Si)—O). This band was sensitive to the content of structural Si and Al. Two intense bands at 906–910

Table 3
Surface area, pore volume and pore diameter of catalyst.

Catalyst	A_{BET}[a] (m^2/g)	V_{tot}[b] (mL/g)	V_{micro}[c] (mL/g)	V_{meso}[d] (mL/g)	D_{avg}[e] (nm)
Raw bauxite	6.99	1.68×10^{-2}	0	1.68×10^{-2}	9.59
IMB[f]	20.14	2.24×10^{-2}	1.98×10^{-3}	2.04×10^{-2}	4.44
MMB	20.4	1.88×10^{-2}	1.87×10^{-4}	1.69×10^{-2}	3.684

[a] BET surface area.
[b] Total pore volume of the surface of catalyst.
[c] Micro pore volume of the surface of catalyst.
[d] Mesopore volume of the surface of catalyst.
[e] Average diameter of pore distributed over the surface of catalyst.
[f] The concentration of precursor was 0.2 mol/L for IMB or MMB.

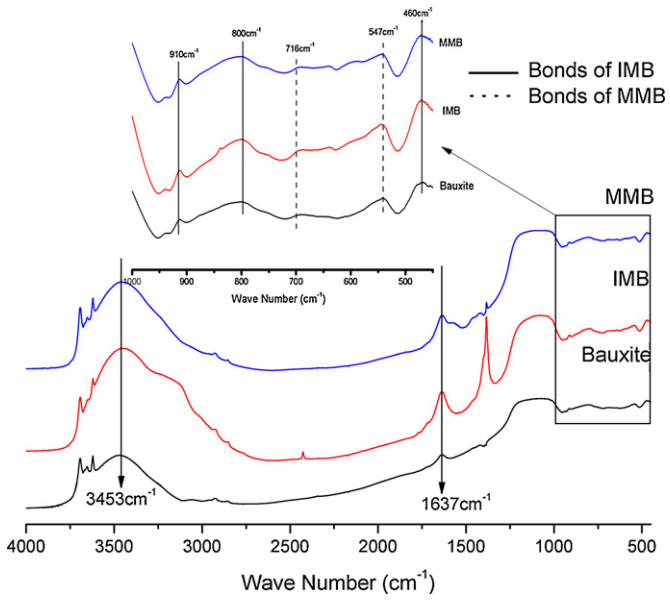

Fig. 9. FT-IR characterization of raw bauxite, IMB and MMB.

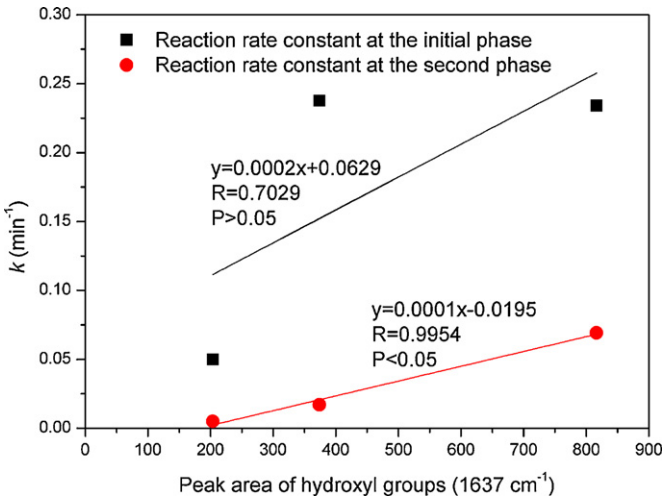

Fig. 11. Effect of surface hydroxyl groups on the catalytic activity for modified bauxite. Experiment conditions were: $[TCA]_0 = 28.2\ \mu g/L$, $[O_3]_0 = 0.62$ mg/L, $[catalyst]_0 = 500$ mg/L, the concentration of precursor was 0.2 mol/L for IMB or MMB, solution pH 6.5 adjusted with phosphate buffer solution, reaction time 30 min.

and 802–806 cm^{-1} were seen for both the raw bauxite and IMB. These were ascribed to goethite (α-FeOOH). Bands at 550 cm^{-1} and 460 cm^{-1} supported the presence of Fe—O bonds, which suggested iron oxide was present. The peak intensity for goethite and Fe—O was stronger in the spectrum of IMB than in that of raw bauxite. This demonstrated that the amount of iron oxide in the catalyst was increased by modification. Two bands at 710 and 547 cm^{-1} were seen in the spectra of both the raw bauxite and MMB. These were ascribed to O—Mn—O bonds, which suggested the presence of manganese oxide.

3.9. Mechanism of catalytic ozonation TCA by modified bauxite

To discuss the role of pore on catalyst in catalytic ozonation, the volume of micropore and mesopore of raw bauxite and modified bauxite, and the reaction kinetic constant in catalytic ozonation have been considered. The relationship between the kinetic constants of the reaction and the pore volume is shown in Fig. 10.

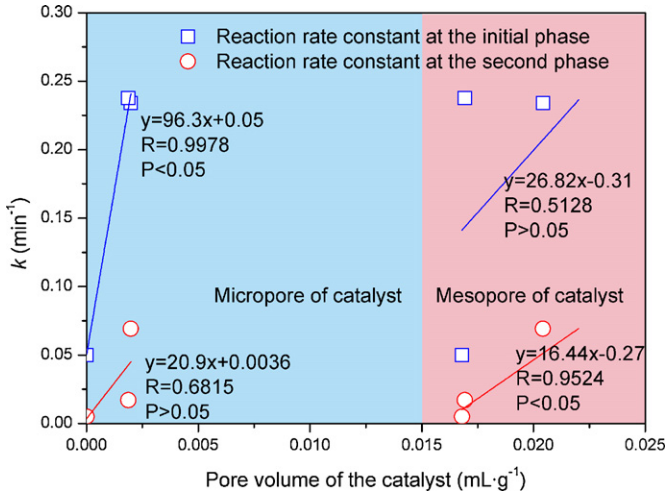

Fig. 10. Effect of pore volume on catalytic activity for modified bauxite. Experiment conditions were: $[TCA]_0 = 28.2\ \mu g/L$, $[O_3]_0 = 0.62$ mg/L, $[catalyst]_0 = 500$ mg/L, the concentration of precursor was 0.2 mol/L for IMB or MMB, solution pH 6.5 adjusted with phosphate buffer solution, reaction time 30 min.

There was a good linear relationship between micropore volume and reaction kinetic constant in the initial reaction ($R = 0.9978$ and $P < 0.05$ in Fig. 10). There was no linear relationship between the reaction kinetic constants in the second reaction and the variation of micropore volume for the R value was so lower ($R = 0.6815$ and $P > 0.05$). Furthermore, as the mesoporous volume increased, the reaction kinetic constants also increased in the second reaction, and a good linear relationship was observed ($R = 0.9524$ and $P < 0.05$). But there was no relationship between mesoporous volume and the reaction kinetic constants in the initial reaction ($R = 0.5128$ and $P > 0.05$). According to results, the reaction of catalytic ozonation could be proposed as below. First, ozone molecules and TCA were adsorbed quickly in the micropores of the catalyst in the initial reaction, and a surface catalytic reaction resulted in ozone decomposition and TCA degradation. The microporous surface increased the probability of collisions among the catalysts, pollutants, and ozone molecules. The direct and indirect oxidation between ozone and TCA was occurred. After that, ozone and TCA diffused over the mesoporous surface of the catalyst. Mesoporous surface was favored for the reaction between ozone and TCA in the second reaction phase.

Surface hydroxyl groups are key for the catalytic ozonation or catalytic ozone decomposition to generate •OH [41]. The relationship between the peak area of surface hydroxyl groups in FT-IR (1637 cm^{-1}) and reaction kinetic constants is shown in Fig. 11. The FT-IR peak area of the surface hydroxyl groups showed a good linear relationship with the second phase reaction kinetic constant ($R = 0.9954$ and $P < 0.05$), and no relationship with the initial reaction ($R = 0.7092$ and $P > 0.05$). The result in Fig. 11 confirmed that surface hydroxyl groups were beneficial for the second phase of the reaction. Therefore, the enhancement of the catalytic activity of modified bauxite in the second phase of the reaction was because of the surface hydroxyl groups. Based on the results for the effect of pore volume on the catalytic activity of modified bauxite in the second phase of the reaction, it was concluded that the mesoporous surface of IMB and MMB was covered by surface hydroxyl groups, which favored the second phase reaction. No relationship between the initial reaction and surface hydroxyl groups suggested that there were less surface hydroxyl groups on the microporous surface. The catalytic reaction initiated by the adsorption of ozone molecules and TCA on the microporous surface dominated the initial reaction, and then ozone and TCA diffused over mesoporous

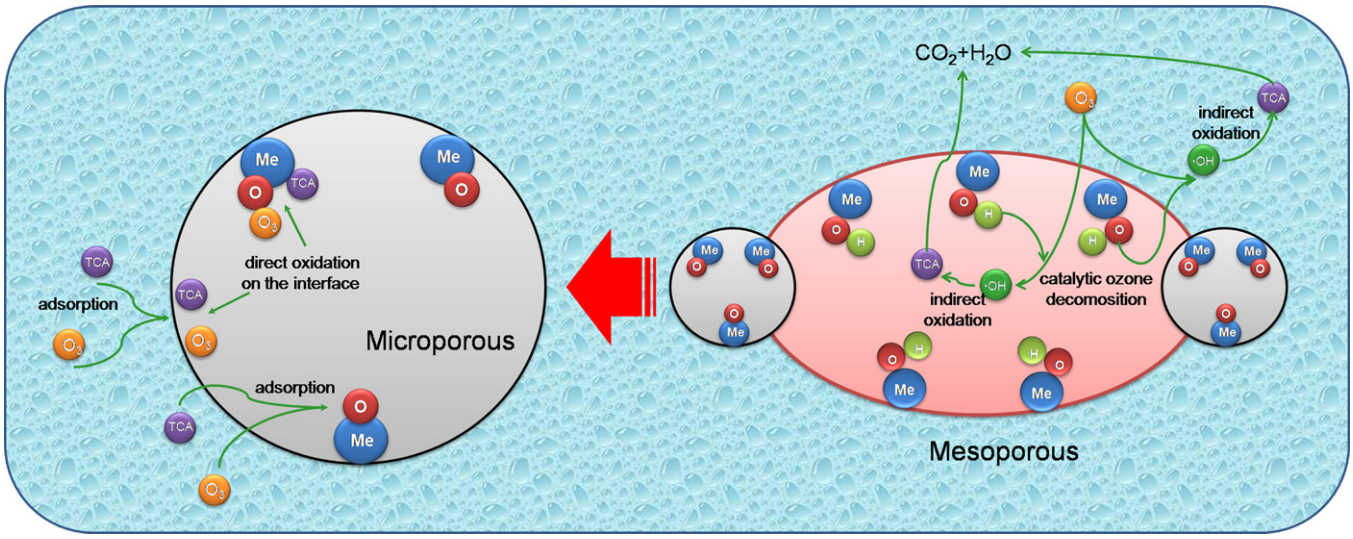

Fig. 12. Proposed catalytic ozonation pathway by modified bauxite.

surface. Surface groups covering the mesoporous surface initialed ozone decomposition to generate •OH dominated the second phase reaction.

In general, the following three pathways have been suggested for catalytic ozonation [34]: (1) chemisorption of ozone on the catalyst surface leading to the formation of active species, which can oxidize the non-chemisorbed organic molecule; (2) chemisorption of organic molecules (associative or dissociative) on the catalyst surface and their further oxidation by gaseous or aqueous ozone; and (3) chemisorption of both ozone and organic molecules and the subsequent interaction between chemisorbed species. In this study, there was a mixed reaction over the surface of catalyst. First, adsorption of both ozone and TCA in the micropores and their subsequent interaction occurred. In micropore of modified bauxite, the direct and indirect reaction occurred between ozone and TCA, resulted in the fast degradation of TCA. Then ozone and TCA were diffused over the mesoporous surface. The chemisorption of ozone on the catalyst mesoporous surface occurred because of the presence of surface hydroxyl groups, which led to the formation of active species (•OH) that could oxidize TCA. A possible reaction mechanism for catalytic ozonation by modified bauxite is proposed and illustrated in Fig. 12.

4. Conclusions

Based on experimental data, the following conclusions can be drawn:

(1) TCA was effectively removed by catalytic ozonation in the presence of IMB or MMB. Iron or manganese oxide modification of the bauxite remarkably enhanced its catalytic activity. For large dissolution of Mn^{2+}, the application of MMB in catalytic ozonation of TCA was not safe.
(2) According to the catalytic ozone decomposition and TBA inhibition experiments, •OH was generated in catalytic ozonation of TCA by IMB or MMB. Modification of the bauxite enhanced the catalytic ozone decomposition to generate •OH. This enhancement was stronger with IMB than with MMB, which could be explained by the difference in the catalytic activities of IMB and MMB.
(3) The reaction mechanism of the modified bauxite catalytic ozonation of TCA was determined by analysis of the surface properties of the modified bauxites, such as the IEP, specific surface area, porous volume and surface groups. In catalytic ozonation, adsorption of both ozone and TCA in the micropores of the catalyst resulted in the subsequent interaction (direct or indirect oxidation) between chemisorbed species. And then, the diffusion of ozone and TCA was occurred on catalyst's mesoporous surface. Surface hydroxyl groups covering the mesoporous surface initialed catalytic ozone decomposition to generated •OH that dominated the degradation of TCA.

Acknowledgements

This work was carried out with the financial support of Research Funds for the Central Universities (no. HJ2010-5), the National Natural Science Foundation of China (no. 51108030) and the Specialized Research Fund for the Doctoral Program of Higher Education (no. 20100014120001), and is supported by China Post Doctoral Science Foundation (20100470216 and 201104060) also supported this research. At last, thanks for the quality improvement of this paper by the anonymous reviewers.

Appendix A. Supplementary data

Supplementary data associated with this article can be found, in the online version, at doi:10.1016/j.apcatb.2012.04.003.

References

[1] L. Maillet, D. Lenes, D. Benanou, P. Le Cloirec, O. Correc, Journal of Water Supply: Research & Technology 58 (2009) 571–579.
[2] N. Park, Y. Lee, S. Lee, J. Cho, Desalination 212 (2007) 28–36.
[3] I. Márquez-Sillero, E. Aguilera-Herrador, S. Cárdenas, M. Valcárcel, Analytica Chimica Acta 702 (2011) 199–204.
[4] C. Prat, E. Besalú, L. Bañeras, E. Anticó, Food Chemistry 126 (2011) 1978–1984.
[5] J. Vestner, S. Fritsch, D. Rauhut, Analytica Chimica Acta 660 (2010) 76–80.
[6] V. Panagiotis, S. Elias, L. Gerasimos, L. Panagiotis, Catalysis Communications 9 (2008) 1987–1990.
[7] F. Qi, B. Xu, Z. Chen, J. Ma, D. Sun, L. Zhang, Separation and Purification Technology 66 (2009) 405–410.
[8] D. Bruce, P. Westerhoff, A. Brawley-Chesworth, Journal of Water Supply: Research & Technology 51 (2002) 183–197.
[9] Chestnutt Jr., E. Thomas, M.T. Bach, D.W. Mazyck, Water Research 41 (2007) 79–86.
[10] S. Lalezary, M. Pirbazari, M.J. McGuire, Journal of the American Water Works Association 78 (1986) 62–69.
[11] C. Fabrellas, L. Matia, F. Ventura, Water Science & Technology 49 (2004) 267–272.
[12] K. Terashima, Water Science & Technology 20 (1988) 275–281.
[13] U. Von Gunten, Water Research 37 (2003) 1443–1463.

[14] F. Qi, B. Xu, Z. Chen, J. Ma, D. Sun, L. Zhang, F. Wu, Journal of Hazardous Materials 168 (2009) 246–252.
[15] C. Pereira, L. Gil, L. Carriion, Radiation Physics and Chemistry 76 (2007) 729–732.
[16] J. Ma, N.J.D. Graham, Water Research 34 (2000) 3822–3828.
[17] F.J. Beltrán, F.J. Rivas, R. Montero-de-Espinosa, Applied Catalysis B: Environment 39 (2002) 221–231.
[18] M. Matheswaran, S. Balaji, S.J. Chung, I.S. Moon, Catalysis Communications 8 (2007) 1497–1501.
[19] F. Qi, Z. Chen, B. Xu, Z. Xu, Journal of Water Supply: Research & Technology 57 (2008) 427–434.
[20] F. Qi, B. Xu, Z. Chen, J. Ma, Water Environment Research 81 (2009) 592–597.
[21] T. Zhang, W. Chen, J. Ma, Z. Qiang, Water Research 42 (2008) 3651–3658.
[22] T. Zhang, C. Li, J. Ma, H. Tian, Z. Qiang, Applied Catalysis B: Environment 82 (2008) 131–137.
[23] L. Yang, C. Hu, Y.L. Nie, J.H. Qu, Environmental Science and Technology 43 (2009) 2525–2529.
[24] J. Ma, M.H. Sui, T. Zhang, Water Research 39 (2005) 779–786.
[25] S. Xing, C. Hu, J. Qu, H. He, M. Yang, Environmental Science and Technology 42 (2008) 3363–3368.
[26] M. Sui, L. Sheng, K. Lu, F. Tian, Applied Catalysis B: Environment 96 (2010) 94–100.
[27] S. Tong, R. Shi, H. Zhang, C. Ma, Journal of Hazardous Materials 185 (2011) 162–167.
[28] H. Bader, J. Hoigne, Water Research 15 (1981) 449–456.
[29] H.-S. Shin, H.-S. Ahn, Chromatographia 59 (2004) 107–113.
[30] R. Gracia, J.L. Aragues, J.L. Ovelleiro, Water Research 32 (1998) 57–62.
[31] K. He, Y. Dong, L. Yin, A. Zhang, Z. Li, Catalysis Letters 133 (2009) 209–213.
[32] T. Sreethawong, S. Chavadej, Journal of Hazardous Materials 155 (2008) 486–493.
[33] Y. Yang, J. Ma, Q. Qin, X. Zhai, Journal of Molecular Catalysis A: Chemical 267 (2007) 41–48.
[34] B. Kasprzyk-Hordern, M. Ziolek, J. Nawrocki, Applied Catalysis B: Environment 46 (2003) 639–669.
[35] L. Zhao, J. Ma, Z. Sun, X. Zhai, Journal of Hazardous Materials 161 (2009) 988–994.
[36] C.L. Bianchi, C. Pirola, V. Ragaini, E. Selli, Applied Catalysis B: Environment 64 (2006) 131–138.
[37] H.N. Lim, H. Choi, T.W. Hwang, J.W. Kang, Water Research 36 (2002) 219–229.
[38] J. Staehelin, J. Hoigné, Environmental Science and Technology 19 (1985) 1206–1213.
[39] W. Stumm, Chemistry of the Solid–Water Interface, Wiley & Sons Inc., New York, 1992.
[40] Ministry of Health of the People's Republic of China, Standards for drinking water quality (GB5749-2006), 2006.
[41] S. Song, Z. Liu, Z. He, A. Zhang, J. Chen, Environmental Science and Technology 44 (2010) 3913–3918.